The following publication Yuan, J., Gang, W., Xiao, F., Zhang, C., & Zhang, Y. (2024). Two-level collaborative demand-side management for regional distributed energy system considering carbon emission quotas. Journal of Cleaner Production, 434, 140095 is available at https://doi.org/10.1016/j.jclepro.2023.140095.

Two-level Collaborative Demand-side Management for Regional Distributed Energy System considering Carbon Emission Quotas

Abstract:

In demand response programs, users typically modify their energy consumption behavior in response to the grid. Distributed energy systems (DES) also need users' participation to ensure the efficient and stable operation of the system, especially under government-imposed carbon emission quotas. This study proposes a two-level collaborative demand-side management framework that allows users to participate in demand response in distributed energy systems, thereby ensuring that the systems' carbon emission remain within the quota while minimizing the impact on thermal comfort. Firstly, the framework realizes coordination between the supply and demand side. Changing energy use behavior not only reduces the amount of load but also enhances the system's efficiency. Secondly, different type of users can cooperatively adjust their air conditioners according to their load characteristics to achieve optimal overall thermal comfort. The effectiveness of the proposed method is demonstrated in a DES with four types of buildings, evaluated using two indoor thermal environment indexes. Under optimal guidance, the system efficiency is improved by 1.9%. Additionally, there is a 3.3% reduction in carbon emissions, along with a 13.2% improvement in overall indoor thermal comfort compared with unified temperature regulation. This study holds positive implications for users' participation in distributed energy systems to achieve energy saving and carbon reduction.

Keywords:

Distributed Energy System; Demand Response; Air Conditioning System; Carbon Quota; Aggregator

Nomenclature

Abbreviations	
AC	Absorption Chiller
COP	Coefficient of Performance
DE	Differential Evolution Algorithm
DES	Distributed Energy System
DR	Demand Response
HP	Heat Pump
HVAC	Heating, Ventilation and Air Conditioning
ICE	Internal Combustion Engine
IDR	Integrated Demand Response
MAU	Make-up Air Unit
PLR	Part Load Ratio
PMV	Predicted Mean Vote
PV	Photovoltaic
Symbols	
chw	*chilled water*
Cp	*specific heat*
cw	*cooling water*
ele	*electricity*
exh	*exhaust gas*
ext	*external*
f	*function*
int	*internal*
jw	*jacket water*
mec	*mechanical*
P	*power*
Q	*energy*
re	*required*
sh	*shaft*
η	*efficiency*

1 Introduction

Building energy consumption is becoming more significant as occupants' demand for a comfortable indoor environment increases (Gao et al. 2020; outlook 2020; Jin et al. 2022). Moreover, building energy consumption shows big day-night differences due to factors such as work schedules and weather changes. These fluctuations in energy demand present challenges to the stable operation of power grids and distributed energy

systems (Li et al. 2021). Particularly during extreme weather conditions, the peak power exceeds the capacity of the generators, requiring partial power cuts to ensure the adequate power supply of important facilities. This crude method of reducing the load can have a huge impact on the user's daily life, work, and indoor thermal comfort. To address this issue, demand response (DR) strategies that the user adjusts the energy consumption behavior according to the electricity price signal or price incentive are introduced to reduce the peak electricity consumption or energy consumption in a more acceptable way (Kirkerud, Nagel, & Bolkesjø 2021; Energy 2006; Smith & Brown 2015; Yan et al. 2018).

In the context of energy conservation and emission reduction, many countries have proposed the goal of achieving carbon neutrality (Shi et al. 2022). China has proposed the goal of achieving carbon neutrality before 2060. Under this background, the power or heating systems are allocated carbon quotas to limit carbon emissions and promote energy conservation and efficiency improvement (Zhou, Niu, & Lin 2023). The national carbon market also officially began to trade online in July 2021 (Weng et al. 2022), So that carbon reduction can obtain additional profits through carbon trading. As an important energy supply system, the operation of the distributed energy system (DES) under the carbon policy has received extensive attention, in which, energy sharing (Zhang et al. 2023), demand response (Yang et al. 2023), and carbon trading (Li et al. 2022; Zhu & Gao 2023) are often considered. Although the carbon quota is allocated to the energy production side, occupants, as energy consumers, also have an obligation to change their energy utilization behavior to participate in carbon reduction through appropriate demand response program.

There are many ways to change a user's load profile to participate in demand response. Occupants' electricity consumption behavior changes are often required to reduce the peak building energy demand (Afzalan & Jazizadeh 2019; Arteconi et al. 2016). Household appliances such as televisions, clothes washers, kitchen stoves, water heaters, etc. are usually scheduled for demand response (Su, Zhou, & Tan 2020; Yan et

al. 2018; Hafeez et al. 2020). Energy storage and building integrated renewable energy are often optimized as well to increase the flexibility of energy use (Alzahrani et al. 2023). Due to the larger energy consumption proportion of the air conditioning system in buildings (Wang et al. 2019; Xiao et al. 2022), demand response strategies for air conditioning systems have been widely studied for their advantages of large regulating energy and easy adjusting (Romero Rodríguez et al. 2018). Changing the indoor air temperature is a comment and easy way to participate in the demand response program (Amin, Hossain, & Fernandez 2020; Erdinç et al. 2017). By increasing the indoor temperature by 1 ℃, the cooling load of the building can be reduced by around 10% (Hoyt et al. 2005). To realize the optimal temperature setpoint control for energy savings and thermal comfort, a reinforcement learning architecture is proposed to control the whole-building heating, ventilation, and air conditioning (HVAC) systems (Azuatalam et al. 2020). A maximum weekly energy reduction of 22% can be achieved compared to a handcrafted controller. Reducing the cooling or heating load by temporarily increasing the setpoint temperature is an effective way. However, it must be implemented with careful control to reduce its impact on occupants' thermal comfort (Aghniaey & Lawrence 2018).

Adjustment of other parameters of the air conditioning system can also change the energy consumption of the air conditioning system. The control of the chilled water temperature, the on/off control of fans, and the supply air temperature of the HVAC system can be implemented. A study shows that the chilled water supply temperature control provides the largest electrical power reduction in a commercial building (up to 14.2%). The temperature adjustment strategy is preferable for zones with higher heat gains (Christantoni et al. 2016). A temperature & humidity setback strategy for HVAC systems is proposed that adjusts the indoor temperature & humidity simultaneously by adjusting the supply air and water temperature (Yuan et al. 2021). The results show that, compared with the strategy of only adjusting indoor temperature, the peak load reduction can increase by 4.0% and the thermal comfort dissatisfaction can decrease by

2%. These methods can achieve greater energy-saving effects through careful adjustment of air conditioning system parameters, but improve the requirements of system control. Another method that shuts down one or more operating chillers during a DR event called direct load control is used for emergency load shedding requirements. This method can achieve fast load curtailment compare to the method of adjusting from the air conditioning terminal. However, this method requires additional control to prevent the terminal device from misadjusting and making the method ineffective. (Wang, Wang, & Tang 2019; Ran et al. 2020; Tang, Wang, & Shan 2018).

The goal of demand response projects is usually to reduce peak power from the grid. However, unlike air conditioning systems that totally rely on the grid, the energy can be provided by the internal combustion engine, the grid, and renewable energy in distributed energy systems (DES) (Tian et al. 2019). This makes differences in the approach and objective of demand response programs. Integrated demand response (IDR) strategy that switches between the electricity grid and the natural gas grid is a special approach in DES (Sheikhi, Bahrami, & Ranjbar 2015; Wang et al. 2017; Huang et al. 2019). By shifting the energy load from one source to another, the combined use of different types of equipment allows for significant operational flexibility (Mancarella & Chicco 2013). This method can reduce the impact of demand response on users. However, it requires greater redundancy in system design and is not conducive to energy saving and carbon emissions reduction.

The objective of the demand response program in DES is not limited to reducing the peak power from the grid but can be expanded to ensuring the system's carbon emissions restriction and improving energy efficiency in the context of energy conservation and carbon quota for energy producers. A multi-energy collaborative optimization method is proposed for integrated energy systems considering carbon quota and demand response (Guo et al. 2023). The results indicate that participating in DR leads to a reduction of 10.18% and 3.41% in operational costs and carbon emissions. A coordination scheme for electricity and heat interaction among DESs is proposed (Li

& Yu 2020). The system cost and carbon emission is reduced by 1.59% and 2.76% under DR. When carbon tax is taken into account, the cost of the system rises but the carbon emissions drop significantly. In these studies, the overall performance is mainly improved from the perspective of the system, but the demand response is usually only an option to change the load, without considering how the load changes and the impact on users.

In demand response for multiple user participation, in addition to a unified adjustment mode, some rules are usually used to determine the operation of each user's air conditioner. A dynamic priority-based control strategy is proposed for systems with multi-air-conditioning units to reduce the peak load. The distance between the current indoor temperature and the temperature setpoint is used as the priority of the unit to start. By applying the proposed strategy in a gym with four HVAC units, 15% of the peak demand can be reduced while maintaining or lowering energy consumption (Winstead et al. 2020). The power consumption characteristics of industry users, commercial users, residential users, and agricultural users are considered in a two-stage flexible power sales optimization model for electricity retailers. Price-based demand response and incentive-based demand response are applied to the four types of users. The results show that different types of demand responses have different emphases on peak shaving and valley filling, and a combination can achieve the best effect (Yan et al. 2022). Distributed energy systems typically serve multiple types of buildings/users. The cooling load characteristics of different buildings are quite different, such as peak valley difference or proportion of sensible load. These characteristics should be considered in formulating demand response strategies for better performance.

From the above review, air conditioning systems can participate in demand response under different application scenarios, objectives, and methods (Fig. 1). However, existing research on demand response strategies still has the following gaps regarding its application to distributed energy systems:

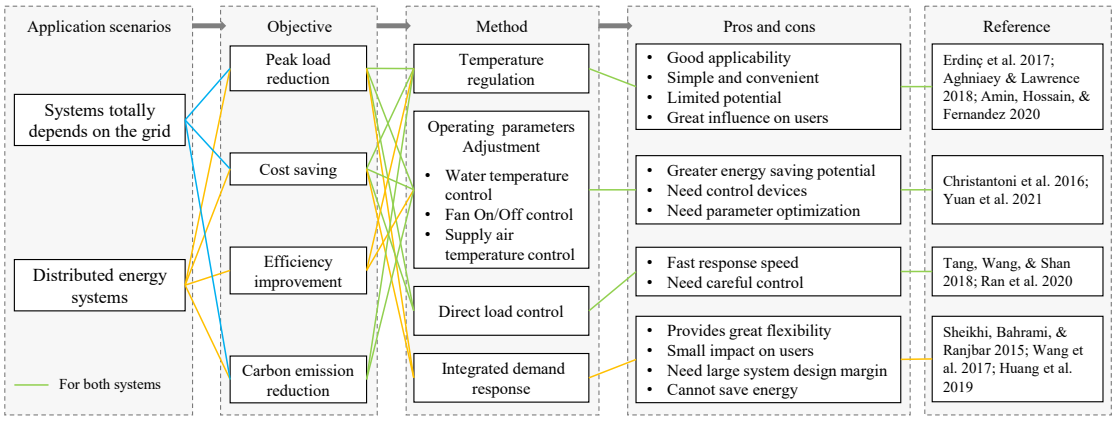

Fig. 1 Application scenarios, objective, and method of demand response in air conditioning systems

- In existing demand response programs, users are usually driven by economic factors so users still do not know what adjustments need to be made to achieve a specific carbon reduction target, especially in the regulation of air conditioning systems. In this situation, there is a need for clear demand response guidance to ensure the effectiveness of demand response and improve users' participation.

- Existing demand response programs are mainly focused on the system that totally depends on the grid. In distributed energy systems, the energy is provided by the internal combustion engine, the grid, and renewable energy. Therefore, the objective of demand response programs is not limited to reducing the peak power of the grid, but can also to improving the efficiency of the distributed energy system and reducing carbon emissions. Therefore, both the energy matching and the system efficiency interaction between the energy supply side and the demand side should be considered.

- There are usually different types of buildings in regional distributed energy systems. Due to their different load characteristics, the load characteristics of various buildings should be considered in the demand response strategy to formulate appropriate operation strategies. Demand response projects with multi-user cooperation should be proposed to achieve a better energy-saving effect and indoor thermal environment.

Therefore, this paper proposes a two-level collaborative demand-side management framework for regional distributed energy systems. The framework aims to provide HVAC adjustment guidance to different users to achieve system carbon emission quota, improve system efficiency, and achieve a better indoor thermal environment. To achieve the two-level collaboration, an aggregator consolidates the information on the supply and demand side and generate optimal guidance through optimization. Three levels of carbon quotas are set as constraints and two indoor thermal environment evaluation indexes are set as objectives in the optimization to verify the effectiveness of the framework under different scenarios.

The following organization of the paper is as follows: The proposed two-level collaborative demand-side management framework, system modeling and optimization are introduced in section 2. A campus is selected for the case study and introduced in section 3. In section 4, the indoor temperature guidance is optimized under three levels of carbon emission quotas and two objectives. In section 5, the significance and limitation of this study are discussed. Finally, conclusions are summarized in section 6.

2 The proposed collaborative demand response framework

The proposed collaborative demand-side management framework is introduced in this section. The framework of the two-level collaboration demand-side management is shown in Fig. 2. The system is modeled in TRNSYS, in which the distributed energy system provides electricity, cooling, and heating energy for different users by consuming natural gas, electricity from the grid, and renewable energy. Occupants can change the indoor temperature setting to change the cooling load to participate in demand response programs. Besides the energy flow between the energy supply side and the demand side, an aggregator realizes the information interaction between the supply side and the users by integrating the system operation data and the information from different buildings. The aggregator is modeled in Python to realize data collection and system optimization.

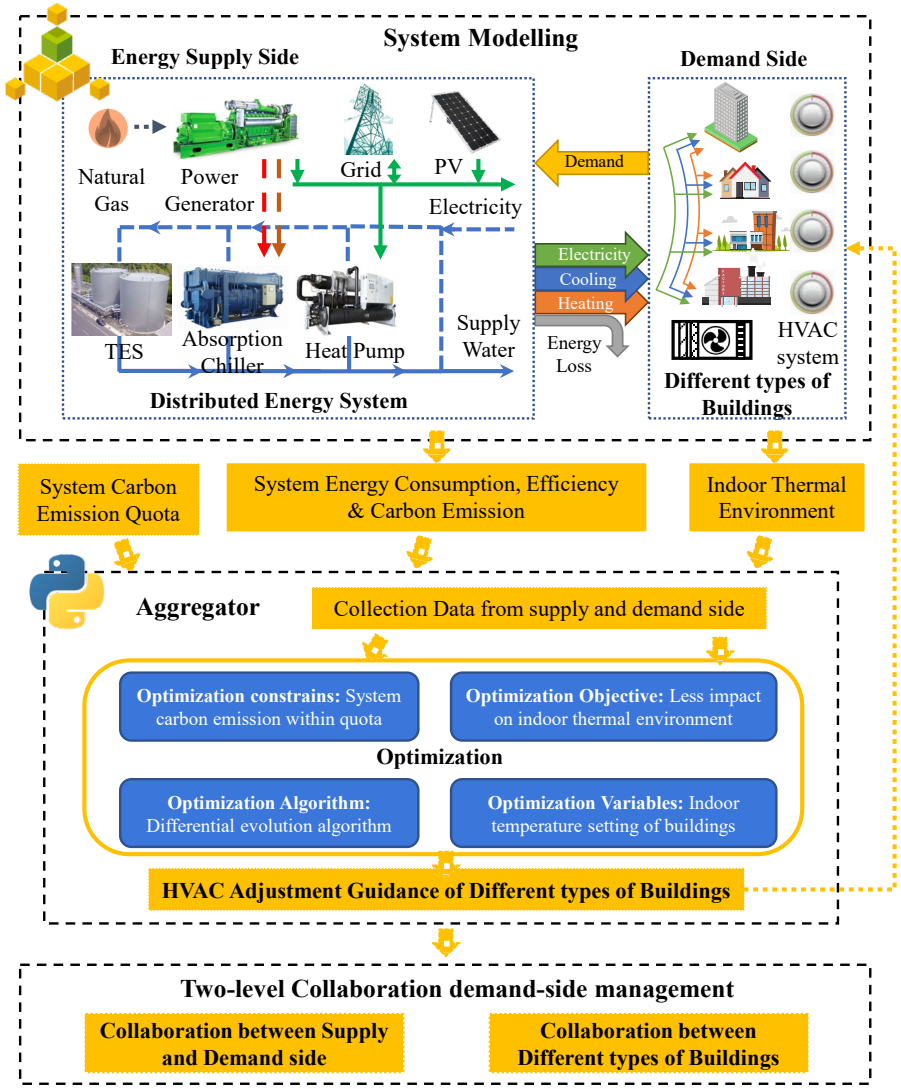

Fig. 2 The proposed collaborative demand-side management framework

2.1 Two-level collaboration demand-side management

Carbon emission quotas are usually allocated to energy producers to limit carbon emissions. The distributed energy systems produce electricity, cooling, and heating energy to users by consuming natural gas. It depends less on the grid, hence the system's carbon emission depends mainly on the supplied energy and system efficiency. In distributed energy systems for many types of buildings, two-level collaboration is required to achieve system carbon emission quota with higher system efficiency and a better indoor thermal environment.

- The first level is to achieve collaboration between the energy supply side and the

demand side. If the energy demand can be reduced and the load profile can also be reshaped to make the system efficiency higher, the system can meet the carbon emission quotas with higher energy production and lower energy loss under higher efficiency. This is beneficial both for the efficiency of the distributed energy system and for the thermal comfort of the occupants.

- The second level is to achieve collaboration between occupants in different types of buildings. Different types of buildings have different patterns of energy use and show different load characteristics. The temperature changes for different buildings and different periods have different influences on the load reduction and indoor thermal environment. If different types of buildings in the distributed energy systems can adjust the indoor temperature cooperatively, the building with higher load reduction and lower influence on the indoor thermal environment by temperature regulation can be adjusted preferentially. A better overall thermal environment of the buildings can be achieved under carbon emission quotas.

An aggregator is used to achieve the two-level collaboration by consolidating the information and generating optimal air conditioning temperature setting guidance. After receiving the system carbon emission quota, the aggregator needs to consolidate information including system operation conditions and building thermal conditions. According to the above information, the aggregator needs to obtain the optimal load profile for the supply side that benefits the system's efficiency and meets the carbon quota. Then the temperature settings for different buildings can be optimized. Under this guidance, the system carbon quotas can be achieved with higher system efficiency due to the reshaping of the building load. A better indoor thermal environment can also be achieved by considering the building load characteristics.

2.2 The distributed energy system and building models

The distributed energy system is modeled in TRNSYS. The internal combustion engine (ICE), photovoltaic (PV), and the grid are used to meet the electricity load. The electricity produced by the PV is firstly used, and the rest part of the electricity load is

met by the ICE. The waste heat produced by the ICE is recovered by the absorption chiller to produce the cooling energy for buildings. The insufficient part is met by the electrical chiller. Excess energy can be stored in the thermal energy storage tank. The chilled water system uses the variable flow system to deliver the cooling energy to the terminal units. The make-up air unit is used to handle the fresh air and send it into the room following the volume of fresh air according to the occupancy. Fan coil units handle the return air to take away the indoor heat gain. The wind speed of the fan coil unit is switched between high, medium, and low speeds according to the cooling load to simulate the user's manual wind speed regulation. The water flow rate is controlled by valves to meet the temperature setpoint. The chilled water system is assumed to be controlled ideally based on temperature differential control (7 ℃) to adjust the operation and calculate the energy consumption of the pumps. The 3D building models are imported to Type 56 and connected to the air conditioning terminal units. Based on the system model, the user's setting of air conditioning systems will directly affect the operation of the energy supply devices, which is used to evaluate the impact of demand response on building cooling load, system operation efficiency, and energy consumption in collaborative demand-side management. The mathematical models of the devices are introduced below:

(1) Internal combustion engine

The internal combustion engine (ICE) calculates the consumed natural gas and the generated waste heat energy according to the electricity load, which is modeled based on Type 907 in TRNSYS. A detailed description of the model can be found in reference (the Solar Energy Laboratory 2017). The input energy of natural gas Q_{re} is calculated in Eq.1~2. Where, $P_{ICE,sh}$ is shaft power, $P_{ICE,out}$ is power output, η_{mec} is mechanical efficiency and η_{ele} is electricity efficiency. The generated waste heat in jacket water Q_{jw} and the exhaust gas Q_{exh} is calculated in Eq.3~4, in which, f_{jw} and f_{exh} are the heat proportion of the jacket water and the exhaust gas. Under different part load ratios, the efficiency of the model will change according to the performance curve

fitted based on the manual. The coefficients are shown in Table A1.

$$Q_{re}=P_{ICE,sh}/\eta_{ele} \quad (1)$$

$$P_{ICE,sh}=P_{ICE,out}/\eta_{mec} \quad (2)$$

$$Q_{jw}=f_{jw}\times(Q_{re}-P_{ICE,sh}) \quad (3)$$

$$Q_{exh}=f_{exh}\times(Q_{re}-P_{ICE,sh}) \quad (4)$$

(2) Absorption chiller

The absorption chiller (AC) calculates the supplied cooling energy by the input waste heat, which is modeled based on our previous work (Yuan et al. 2023). Firstly, the coefficient of performance (COP) is modified by the waste heat and temperature as shown in Eq.5~9. Therefore, the cooling energy supply ability under the current waste heat input can be calculated in Eq.10. Then the needed cooling energy of the users is calculated through the chilled water, as shown in Eq.11. If the needed energy of the chilled water is lower than the cooling supply, the chiller operates at the cooling demand. If the needed energy of the chilled water is higher than the cooling supply, the outlet temperature of the chilled water is recalculated and the COP needs to be re-modified until it converges. Where, plr_{heat} is the part load ratio of input energy, Q_{exh} and Q_{jw} are the energy of the exhaust gas and jacket water, $Q_{chw,AC,supply}$ is the supplied cooling energy, $Q_{chw,AC}$ is needed cooling energy, a_1-c_3 are coefficients to describe the characteristics of the polynomial, which are shown in Table A2.

$$plr_{heat}=(Q_{exh}+Q_{jw})/(Q_{exh.rate}+Q_{jw.rate}) \quad (5)$$

$$COP_{plr}=(a_1\times plr_{heat}^3+a_2\times plr_{heat}^2+a_3\times plr_{heat}+a_4)\times Q_{chw.rate}/(Q_{exh}+Q_{jw}) \quad (6)$$

$$\beta=b_1\times T_{chw,AC,out}^2+b_2\times T_{chw,AC,out}+b_3 \quad (7)$$

$$\gamma=c_1\times T_{cw,AC,in}^2+c_2\times T_{cw,AC,in}+c_3 \quad (8)$$

$$COP_{AC}=COP_{plr}\times\beta\times\gamma \quad (9)$$

$$Q_{chw,AC,supply}=(Q_{exh}+Q_{jw})\times COP_{AC} \quad (10)$$

$$Q_{chw,AC}=C_p \times F_{chw,AC} \times (T_{chw,AC,in}-T_{chw,AC,out}) \quad (11)$$

(3) Heat pump

The electricity consumption of the heat pump (HP) is calculated based on the required cooling demand (Zhang et al. 2020). The outlet temperature of the chilled water is presupposed, and the needed cooling energy, part load ratio (PLR), and power consumption can be calculated according to Eq.12~17. If the PLR is larger than 1, the chilled water outlet temperature is recalculated to keep the cooling energy within the capacity. Where, $Q_{\mathrm{chw,HP}}$ is the cooling energy. $F_{chw.HP}$ is water flow rate. $T_{chw,return}$ and $T_{chw,HP,out}$ are return and supply water temperature. CAP_{full} is the capacity of the HP. P and P_{noc} are HP power under actual and nominal conditions. $CAPFT$, $EIRFT$, and $EIRFPLR$ are used to correct heat pump power under different conditions. $T_{cw,HP,in}$ is the inlet cooling water temperature. e_1–g_3 are coefficients that are fitted based on the performance curve of a heat pump as shown in Table A3.

$$Q_{chw,HP}=C_p \times F_{chw.HP} \times (T_{chw,return}-T_{chw,HP,out}) \quad (12)$$

$$plr=Q_{chw,HP}/CAP_{full} \quad (13)$$

$$P=P_{noc} \times CAPFT \times EIRFT \times EIRFPLR \quad (14)$$

$$CAPFT=CAP_{full}/CAP_{noc}=e_1+e_2 \times (T_{chw,HP,out}/T_{chw,HP,out,noc})$$

$$+e_3 \times (T_{cw,HP,in}/T_{cw,HP,in,noc}) \quad (15)$$

$$EIRFT=(P_{full}/CAP_{full})/(P_{noc}/CAP_{noc})=f_1$$

$$+f_2 \times (T_{chw,HP,out}/T_{chw,HP,out,noc})+f_3 \times (T_{cw,HP,in}/T_{cw,HP,in,noc})$$

$$+f_4 \times (T_{chw,HP,out}/T_{chw,HP,out,noc})^2+f_5 \times (T_{cw,HP,in}/T_{cw,HP,in,noc})^2 \quad (16)$$

$$EIRFPLR=P/P_{full}=g_1 \times plr^2+g_2 \times plr+g_3 \quad (17)$$

(4) Cooling coil

The model of the cooling coil is used in the fan coil unit and the make-up air unit (MAU) for the heat exchange between moist air and water. The chilled water coil model

(Partially Wet) Type 124 in TRNSYS is used, which is detailed in the reference (the Solar Energy Laboratory 2017). As shown in Eq.18~24, the designed coefficient of heat transfer UA is calculated based on the parameter settings. Then, the UA values in operation are adjusted based on the inlet conditions. Where, the heat transfer rate Q_{MAU} is calculated by the enthalpy-based overall heat transfer coefficient UA_h and the enthalpy difference. C_p is the specific heat. UA_{ext} and UA_{int} are the overall heat transfer coefficient of the air side and the liquid side, which are adjusted by the flow rate and inlet temperature of the air and fluid m_{air}, $T_{air,in}$, m_{liq}, $T_{liq,in}$ on the operating conditions.

$$Q_{MAU}=UA_h\times(h_{out}-h_{in}) \tag{18}$$

$$UA_h=UA/C_p \tag{19}$$

$$UA=1/(1/(UA_{ext})+1/(UA_{int})) \tag{20}$$

$$UA_{ext}=UA_{ext,rated}\times x_a\times(m_{air}/m_{air,rated})^{0.8} \tag{21}$$

$$x_a=1+0.004769\times(T_{air,in}-T_{air,in,rated}) \tag{22}$$

$$UA_{int}=UA_{int,\ rated}\times x_w\times(m_{liq}/m_{liq,rated})^{0.85} \tag{23}$$

$$x_w=1+(0.014/(1+0.014\times T_{liq,in,rated}))\times(T_{liq,in}-T_{liq,in,rated}) \tag{24}$$

(5) Fan

The power consumption of the fans is calculated in the fan model, which uses Type 744 in TRNSYS (the Solar Energy Laboratory 2017). As shown in Eq.25, the power consumption of the fan is modified according to the cubic relation of the flow rate. Where, P_{fan} is fan power, $P_{fanrate}$ is the rated fan power, m_{air} is the air flowrate and m_{rated} is the rated air flowrate.

$$P_{fan}=P_{fanrate}\times(m_{air}/m_{rated})^3 \quad (25)$$

(6) Pump

The pump model calculates its power consumption according to the pressure difference and flow rate. The variable speed pump model Type 742 in TRNSYS is used (the Solar Energy Laboratory 2017). As shown in Eq.26 the pump power P_{pump} is calculated by the work done in pumping the fluid W_{pump}, the electric efficiency η_{motor}, and the pump efficiency η_{pump}. The work done by the pump is calculated by the pressure difference Δp, fluid flowrate m_{fluid} and the fluid density ρ_{fluid} as shown in Eq.27.

$$P_{pump}=W_{pump}/\eta_{pump}/\eta_{motor} \quad (26)$$

$$W_{pump}=\Delta p\times m_{fluid}/\rho_{fluid} \quad (27)$$

2.3 System optimization

To obtain the optimal user temperature regulation guidance in the aggregator, the differential evolution (DE) algorithm is used to find the optimal temperature regulation guidance for different users, which is implemented by the Geatpy algorithm toolbox (Jazzbin 2020). In the model, the variables are supplied by the DE algorithm in Python and transferred to TRNSYS for system simulation. The simulation results are then sent back to Python for further judgment. After the optimization, the optimal daily temperature guidance for collaborative demand side management for different types of buildings can be obtained. In the Geatpy algorithm toolbox, the soea_DE_rand_1_bin algorithm is used. The population is 80 and the maximum generation is 100. Other parameters are left as default.

(1) Constraints

The limitation that the carbon emission of the DES must be within the quotas is modeled

as a constraint. The energy balance constraint is already satisfied in the system model in TRNSYS. Carbon quotas are set based on the system's basic carbon emission, which is calculated based on indoor temperature settings of 26 ℃ and without demand response. Since this study mainly focuses on the indoor temperature settings that only influence the cooling load, the carbon emission of the cooling system is separated and used for quota calculation. As shown in Eq.28, the carbon emission of the cooling system is calculated based on the total carbon emission of the system and the proportion of the electricity consumption of the cooling system to the total electricity consumption. Where, V_{gas} is consumed natural gas (m^3), E_{grid} is electricity from the grid (MWh). ϑ_{gas} and ϑ_{grid} are carbon emission factors of natural gas and the grid, which are selected as 1.96 t/m^3 and 0.581 t/MWh, respectively (China 2022). E_{HP}, E_{pump}, E_{fan}, and E_{total} are electricity consumption of the heat pumps, water pumps, fans, and system total electricity consumption. Three levels of carbon quotas are set as constraints based on a reduction in basic cooling system carbon emissions of 10%, 20%, and 30% respectively. Because the relationship between the indoor temperature set points with carbon emission is hard to describe directly, all cases are calculated first to determine whether their carbon emissions are within the range. Cases with carbon emissions that meet the quota will be left for further consideration. This function can be achieved through a parameter "CV" in the Geatpy algorithm toolbox.

$$CE_{cooling}=(V_{gas}\cdot\vartheta_{gas}+E_{grid}\cdot\vartheta_{grid})\frac{E_{chiller}+E_{pump}+E_{fan}}{E_{total}} \quad (28)$$

(2) Optimization objective

The objective of the optimization is minimizing the impact on the indoor thermal environment, in which average predicted mean vote (PMV) and average occupancy-weighted PMV (Occ-PMV) are used. PMV is an evaluation index of occupants' thermal response, in which +3 means too hot and -3 means too cold. The PMV relates to the imbalance between the actual heat flow from the body in a given environment and the heat flow required for optimum comfort at the specified activity (ASHRAE 2017). The

PMV is calculated in the Type 56 multizone building model in TRNSYS based on ISO 7730 (2005), considering clothing factors, metabolic rate, and external work. The daily average PMV of different buildings is calculated in Eq.29, in which n is the number of buildings, i represents the i^{th} building and j is the hour. Considering building area differences, higher weight is given to buildings with large floor areas. Occ-PMV is obtained by weighting PMV according to occupancy as shown in Eq.30. Where, $Occ_{i,j}$ is the occupancy (between 0 and 1) of the i^{th} building in hour j. The indoor thermal environment can be guaranteed preferentially during periods with higher occupancy when using Occ-PMV.

$$PMV_{ave} = \frac{1}{24n} \sum_{i=1}^{n} \sum_{j=1}^{24} (Area_i / Area_{total} \times PMV_{i,j}) \quad (29)$$

$$Occ\_PMV_{ave} = \frac{1}{24n} \sum_{i=1}^{n} \sum_{j=1}^{24} (Occ_{i,j} \times Area_i / Area_{total} \times PMV_{i,j}) \quad (30)$$

(3) Optimization variables

In the optimization model, the indoor temperature setpoints of the four types of buildings in each hour are optimization variables. For simplicity, the temperature setpoint of each room during a period is merged into one variable. Each building uses 5 variables to represent temperature setpoints during 23:00~6:00, 7:00~11:00, 12:00~13:00, 14:00~18:00, and 19:00~22:00, respectively. In this way, there are 20 variables for the daily demand response guidance for 4 types of buildings. The value of each variable is an integer between 25 ℃ and 28 ℃.

(4) Evaluation index

To analyze optimization results, Load_PMV index and Load_Occ_PMV index are proposed. The Load_PMV index is the cooling load reduction under unit PMV variation, which is calculated as Eq.31. $Load_{i,j}^{T}$ is the cooling load of the i^{th} building in tome j with an indoor temperature of T. The larger value means that the cooling load can be reduced with less effect on the occupant's comfort. Load_ Occ_PMV index pays more attention to the indoor thermal environment when the occupancy is higher. As shown

in Eq.32, in the Load_ Occ_PMV index, indoor PMV is given higher weight when the occupancy is high. These two evaluation indexes can be used to analyze the trend of the optimal temperature guidance.

$$Load\_PMV_{i,j}=(Load_{i,j}^{T}-Load_{i,j}^{26})/(PMV_{i,j}^{T}-PMV_{i,j}^{26}) \quad (31)$$

$$Load\_Occ\_PMV_{i,j}=(Load_{i,j}^{T}-Load_{i,j}^{26})/[Occ_{i,j}\times(PMV_{i,j}^{T}-PMV_{i,j}^{26})] \quad (32)$$

3 Case study

A campus in the hot summer and cold winter area in China is selected for the case study. The gross floor area of the buildings is approximately 478600 m^2, with the air conditioning system covering 70% of the area. Four types of buildings with four typical building load characteristics are selected as shown in Fig. 3. In dormitories (D) and teaching buildings (T), the occupants' density is high, resulting in a greater proportion of the latent cooling load due to the larger number of occupants and fresh air volume. Conversely, in residential (R) and office buildings (O) the density of occupants is relatively low and the heat gain of equipment is larger, resulting in a higher sensible cooling load. From another dimension, office and teaching buildings have a higher cooling load during the day as they are primarily occupied during that time. In contrast, the cooling load of the dormitory and the residential show less difference between day and night. The diverse load characteristics observed in these dimensions provide valuable insights into the relationship between load characteristics and temperature regulation rules in demand response management.

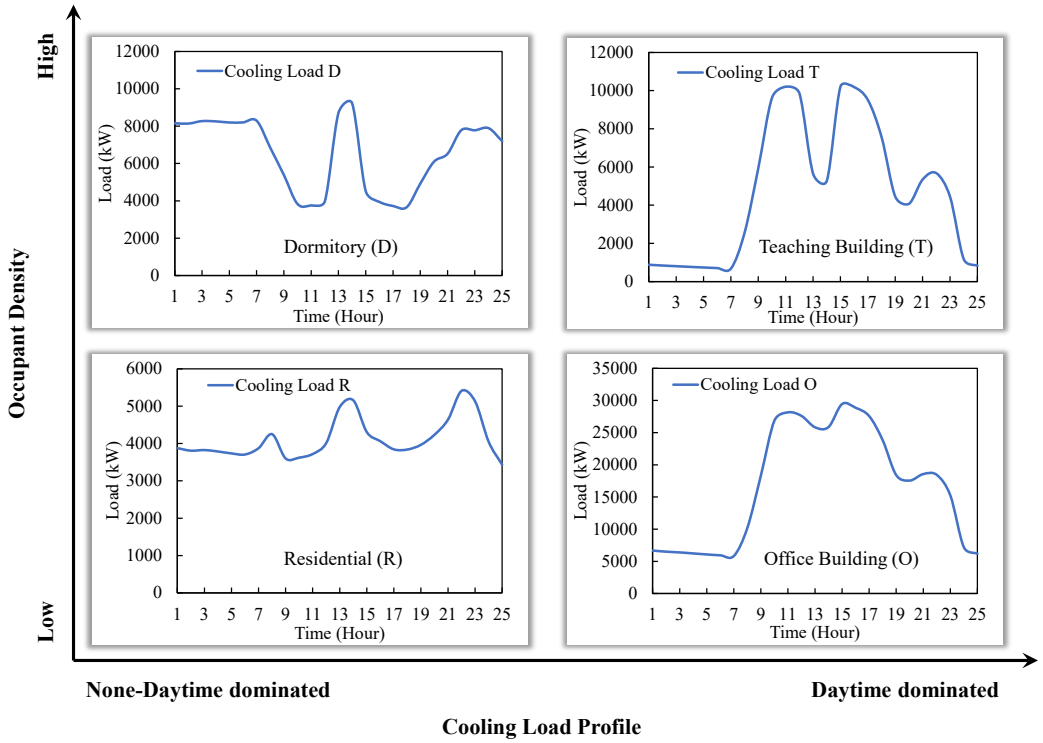

Fig. 3 Cooling load of the four types of buildings

The annual electricity, cooling, and heating load are calculated under the indoor temperature of 26 ℃ and relative humidity of 60% (Fig. 4). The peak electricity, cooling, and heating load is 26038 kW, 55270 kW, and 20347 kW, respectively. Three ICEs with 9500 kW, three absorption chillers of 7400 kW, and four heat pumps of 7735 kW are selected to meet the load. On the demand side, each type of building is represented by a room model and multiplied to calculate the total load of the buildings. The design of the terminal device of the HVAC system is shown in Table 1. Fan coil units are selected according to the indoor load of each building model, and MAUs are selected according to the cooling demand of handling the fresh air.

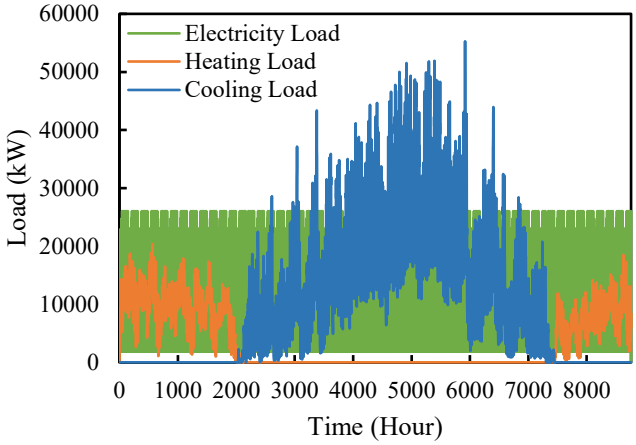

Fig. 4 Annual electricity, cooling, and heating load of the DES

Table 1 HVAC system terminal equipment design

Building Types	Dormitory (D)	Teaching Building (T)	Office (O)	Residential (R)
Number of buildings	93	5	42	134
Fan coil unit				
Unit number in each building model	26	52	40	12
Cooling capacity (kW)	2.13	16.07	12.94	3.26
Sensible cooling capacity (kW)	1.43	9.76	9.52	2.37
Air flowrate (m3/h)	330	2020	2040	500
Water flowrate (kg/s)	0.07	0.55	0.44	0.11
Make-up air unit				
Unit number in each building model	1	3	2	1
Cooling capacity (kW)	99.6	703	252.2	24.2
Sensible cooling capacity (kW)	40	284.3	101.3	9.75
Air flowrate (m3/h)	6000	45000	15000	1500
Water flowrate (kg/s)	3.4	24.0	8.6	0.8

4 Results and analyses

The performance of the system is simulated and analyzed. Firstly, the characteristics of the system supply and demand side under different indoor temperatures are analyzed. Then, guidance under three levels of carbon quotas is optimized and discussed. Finally, considering per capita thermal comfort, different evaluation index is used in the

optimization.

4.1 Characteristics analysis of the system supply and demand side

The operation of the distributed energy system in the unified temperature regulation is analyzed. When the indoor temperature of each building is set to 26 ℃ as shown in Fig. 5, the peak cooling load of the DES is around 47900 kW. The cooling load is fulfilled by the absorption chiller (AC) and the heat pumps (HP). Low electrical load and high PV output decrease the power generated by the ICEs, resulting in reduced cooling produced by the absorption chiller. The electricity balance figure demonstrates that the internal combustion engine (ICE), photovoltaic (PV), and the grid meet the total electricity demand including the electricity demand of the buildings as well as the electricity consumption of the HPs, pump, and fans. The ICEs produce the majority of the electricity load. During periods of high solar radiation, the power of the ICEs can be reduced by 42%.

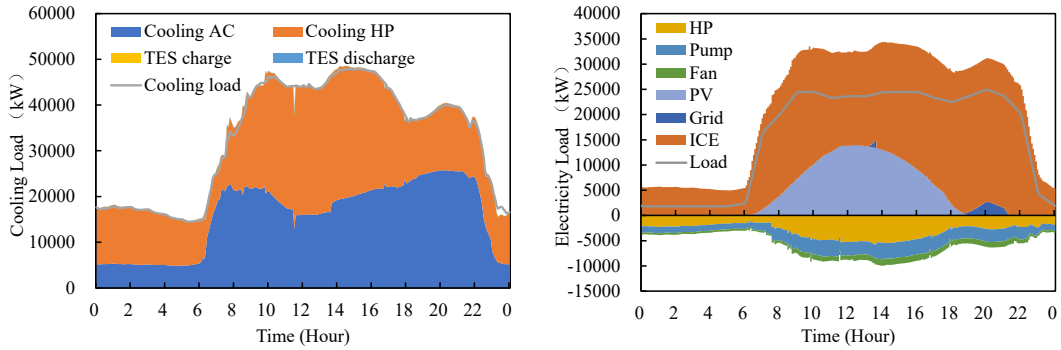

(a) System cooling energy balance (b) System electricity balance

Fig. 5 System cooling energy and electricity balance

The impact of different temperature settings is analyzed in Fig. 6. By increasing the indoor temperature from 26℃ to 27℃ and 28℃, the total carbon emission reduction ratio of the system is 5.6% and 10.3%. These reductions are primarily due to the cooling system emitting less carbon. Consequently, the carbon emission reduction ratio of the cooling system increases to 17.3% and 32.5%. From Fig. 6 (b), as the indoor temperature rises from 26℃ to 27℃ and 28℃, the cooling load reduction ratio is 12.1% and 24.4%. Additionally, as the indoor temperature increases (from 26℃ to 28℃), the

system's primary energy efficiency slightly improves, rising from 84.5% to 85.4%, contributing to further carbon emission reduction.

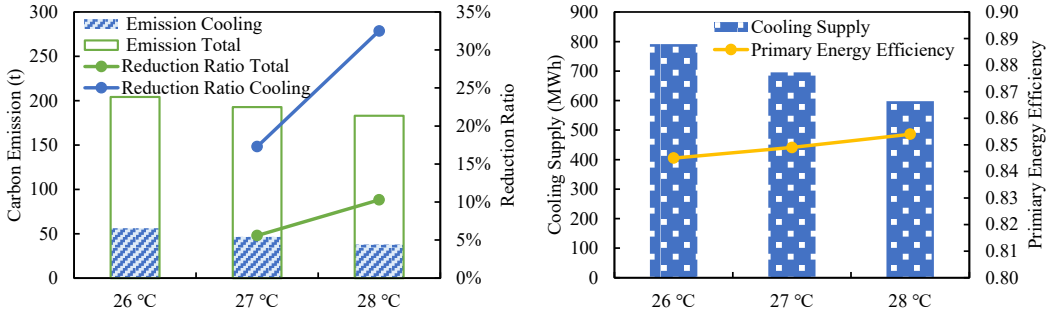

(a) Environmental performance (b) Energy and efficiency performance

Fig. 6 System performance under different indoor temperatures

The cooling load of the four types of buildings is shown in Fig. 7, the cooling load of the office buildings (O) accounts for over 60% of the total cooling load in the daytime because of its large area proportion. Additionally, the cooling load of the office building and the teaching building (T) shows a large night and day difference. In contrast, the fluctuation in the cooling load of the residential buildings (R) and dormitories (D) is relatively minor. This difference is primarily attributed to occupants' activity schedules.

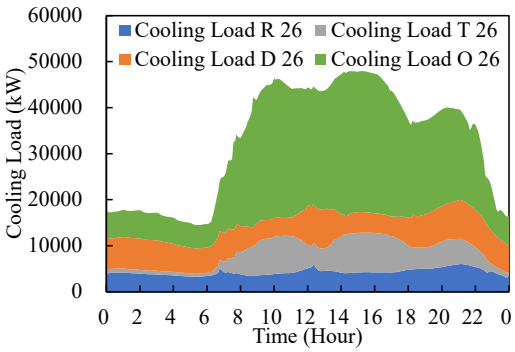

Fig. 7 Cooling load of four types of buildings

The indoor thermal environment of the four types of buildings is illustrated in Fig. 8. The actual indoor temperatures of all the buildings fluctuate around the temperature setpoint (26 ℃). However, the relative humidity and the PMV of the building are different due to moisture differences and the lack of precise humidity control. The dormitories and teaching buildings have higher indoor relative humidity (70%) due to

high occupancy density. In contrast, office buildings and residential buildings maintain an indoor humidity level of around 60% most of the time, as they have more electronic equipment.

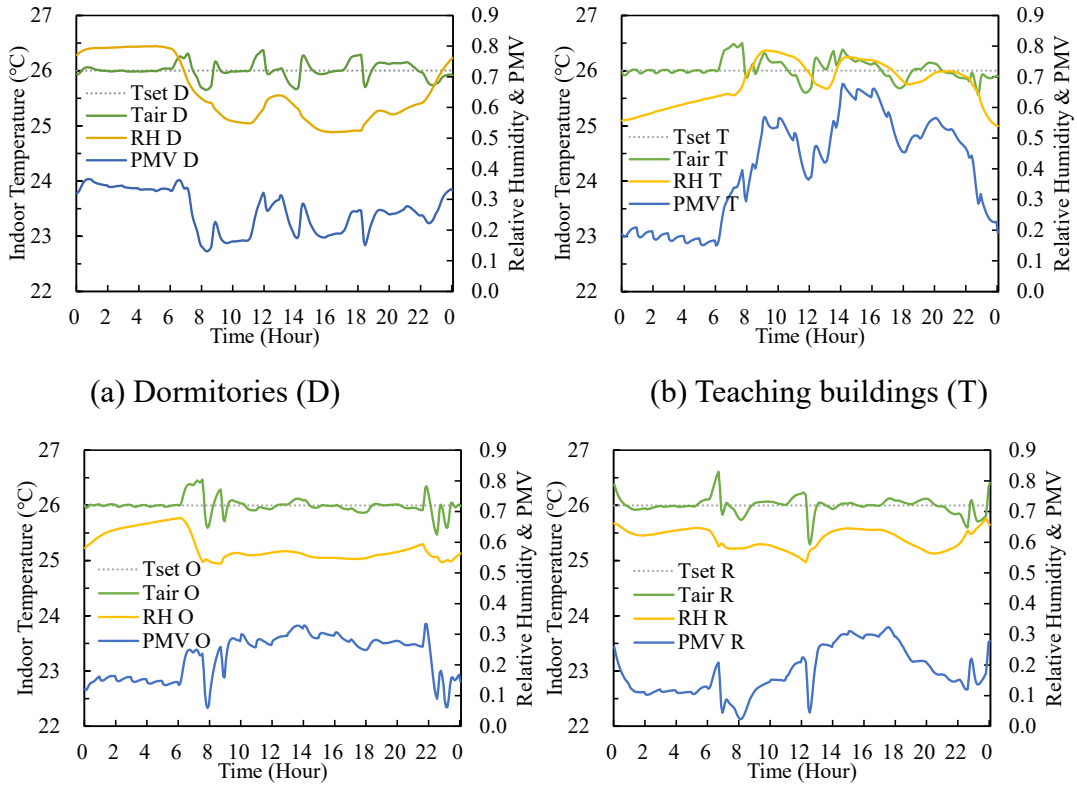

(a) Dormitories (D) (b) Teaching buildings (T)

(c) Office buildings (O) (d) Residential buildings (R)

Fig. 8 Indoor thermal environment of four types of buildings

Due to variations in the cooling load composition across different types of buildings, the cooling load under different indoor temperature setpoints is compared. As shown in Fig. 9, the daily cooling load reduction of four types of buildings is different with the indoor temperature increasing from 26 ℃ to 28 ℃. Adjusting the indoor air temperature in office buildings has the lowest load reduction effect. Increasing the indoor temperature to 28°C results in a decrease of 20.8% and 22.8% in sensible and latent heat loads, respectively. The reason may be that the equipment load of office buildings accounts for a large proportion, which is not sensitive to indoor temperature. In contrast, the cooling load variation for dormitories, and residential buildings are larger under different indoor temperatures. Teaching buildings have the highest occupancy density. Consequently, teaching buildings have the highest proportion of latent cooling load. As

a result, teaching buildings achieve the highest reduction in latent cooling load but a relatively lower reduction in sensible cooling load. This means that adjusting the air-conditioning system of different types of buildings can achieve different energy-saving effects.

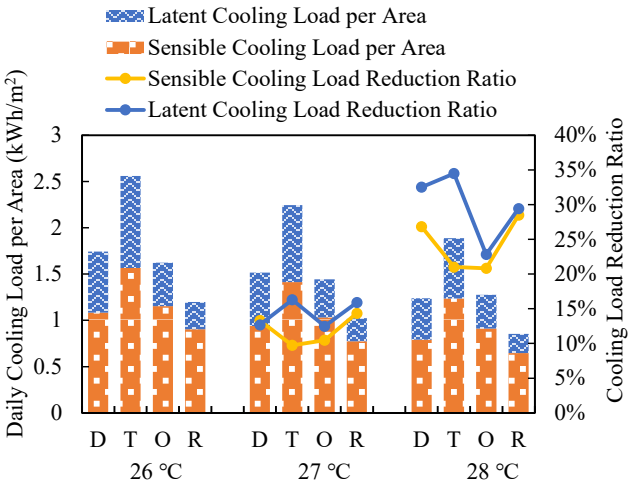

Fig. 9 Cooling load of four types of buildings under different indoor temperatures

Load reduction differences also varied at different hours. Whenever the room temperature is adjusted, the PMV changes are similar but the load changes are different. Consequently, the Load_PMV index is utilized to evaluate the cooling load reduction under unit PMV variation. The larger value means that the cooling load can be reduced with a smaller impact on the occupant's comfort, which should be considered in the demand response prioritized. Fig. 10 illustrates significant differences in the index among different buildings and time intervals. During the early morning period (0:00~6:00), the Load_PMV index of dormitories is higher. In the daytime, the teaching building has the highest Load_PMV (higher than 80). The index for office buildings is stable throughout the day, generally below 40. The index for residential buildings is higher in the evening. Adjusting temperature during the period with a higher Load_PMV index should be given higher priority in demand response strategies. Understanding this characteristic can facilitate the implementation of collaborative demand-side management for multiple users.

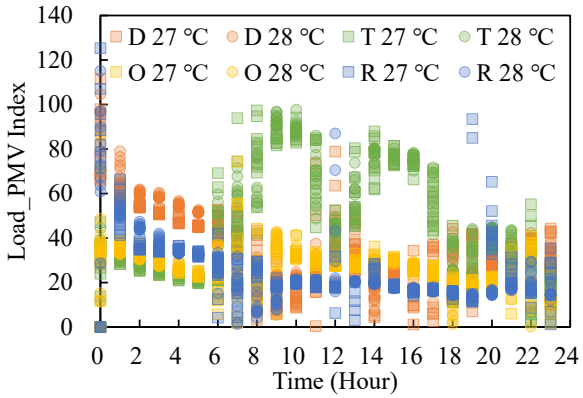

Fig. 10 Load_PMV index of four types of buildings under different indoor temperatures

4.2 Optimal guidance under different carbon quotas

The proposed demand-side management optimization framework aims to optimize the indoor temperature setpoint of each building to minimize the impact on users with the goal of achieving carbon emission quotas. Based on the reference case with 26 ℃ indoor set temperature for all buildings, 10%, 20%, and 30% of three carbon reduction targets were set and the indoor temperature setpoints are optimized. The three scenarios are named PMV_10%, PMV_20%, and PMV_30%. The optimized indoor air temperature setpoints for four types of buildings in the PMV_10% scenario are shown in the first row in Fig. 11. In dormitory buildings, the indoor air temperature is increased to 28 ℃ during 0:00~7:00 and 19:00~0:00, while it is reduced during 12:00~14:00. In teaching buildings, the indoor temperature is increased to 28 ℃ during 7:00~12:00 and 14:00~23:00. The temperature increase in the office buildings is small, the temperature setpoint is reduced to 25 ℃ in the day time. In residential buildings, the temperature of the room rises to 28 ℃ primarily in the afternoon and evening. The temperature settings for each building in the PMV_20% and PMV_30% scenarios have the same trend as the PMV_10% scenario, but the duration of the high-temperature setting increases. The results indicate that different types of buildings should collaboratively adjust their temperature settings based on their characteristics.

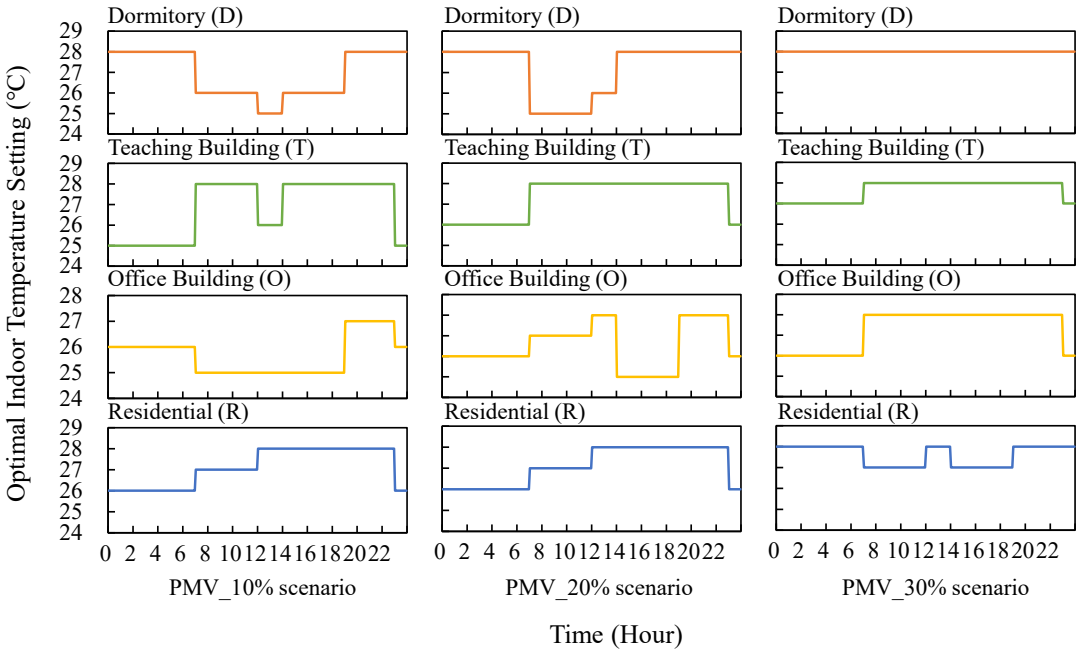

Fig. 11 Optimal indoor temperature guidance in three carbon quota scenarios

Under the above optimal temperature setting guidance, the system performance is compared in terms of the environment, energy, efficiency, and thermal comfort aspects. As shown in Fig. 12 (a), the carbon emission of the cooling system is 56.2 t under the reference scenario (26 ℃). With the reduction of the cooling carbon reduction, the total carbon emission reduction can reach 3.6%, 6.4%, and 9.8% in three scenarios. Compared with the unified temperature setting scenarios, the system carbon emission in the PMV_10% scenario is between the 26 ℃ and 27 ℃ scenarios. the system carbon emission in PMV_20% and PMV_30% scenario is between the 27 ℃ and 28 ℃ scenarios. From energy performance in Fig. 12 (b), the supplied cooling energy is reduced by 5.4%, 11.9%, and 20.7% under PMV_10%, PMV_20%, and PMV_30% scenarios. The collaboration between the demand and supply sides results in the primary energy efficiency of 85.5%, 86.4%, and 85.8% in PMV_10%, PMV_20%, and PMV_30% scenarios respectively, surpassing the highest efficiency achieved in unified temperature scenarios (85.4%). The improved system efficiency reduces the energy loss from the supplied side, resulting in more energy being available for users. This, in turn, enhances user thermal comfort. From the indoor environment in Fig. 12 (c), although different scenarios have different carbon emissions and indoor environment, the

average PMV in the PMV_20% scenario is 0.46, which is 13.2% lower than the 27℃ scenario (0.53) with 3.3% lower carbon emissions. Therefore, the optimal scenario has a better indoor thermal environment with lower carbon emissions compared with unified temperature regulation.

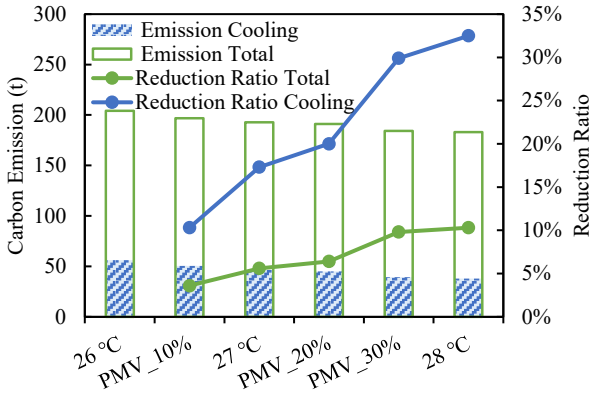

(a) Environmental performance under different scenarios

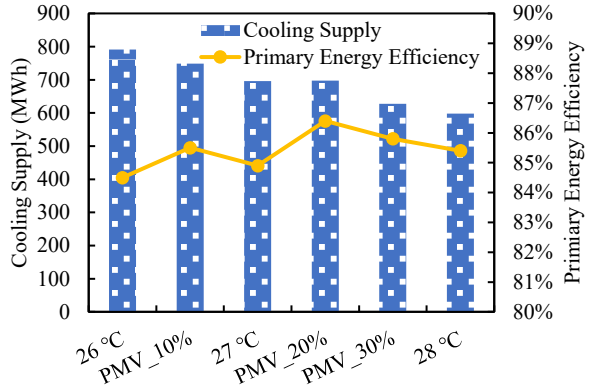

(b) Energy and efficiency performance under different scenarios

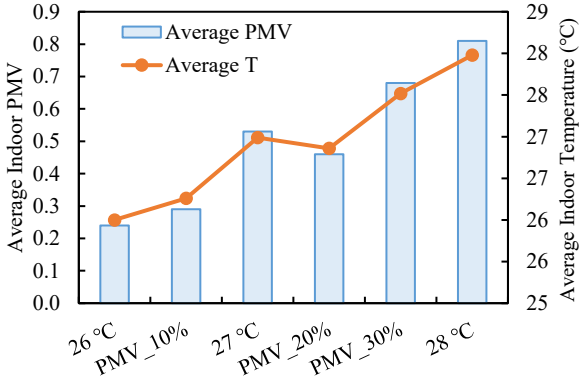

(c) Indoor thermal environment under scenarios

Fig. 12 System performance under different scenarios

584 Optimal temperature settings vary based the characteristics of various types of buildings.
585 Due to the higher occupant density in dormitories and teaching buildings, the two types
586 of buildings have greater load reduction as the indoor temperature increases,
587 particularly during occupant hours. As a result, the temperature settings of the two types
588 of buildings are prioritized for increases during occupant hours. This trend is further
589 supported by the Load_PMV index. Fig. 13 shows the duration of different buildings
590 to increase the indoor temperature and the average PMV index. When 10% of the
591 cooling carbon emission is reduced, the indoor temperature is set to 28 ℃ for over 12
592 hours in dormitories and teaching buildings. Only 4 hours is set to 27 ℃ in office
593 buildings. Eight hours is set to 28 ℃ and 5 hours is set to 27 ℃ in residential buildings.
594 The time period with the temperature adjusted to 28 ℃ is associated with a higher
595 average Load_PMV index. The results demonstrate a strong correlation between the
596 optimal temperature settings and the Load_PMV index. The indoor temperature
597 increases preferential during the time with a higher Load_PMV index to achieve the
598 emission reduction target with minimal thermal comfort impact.

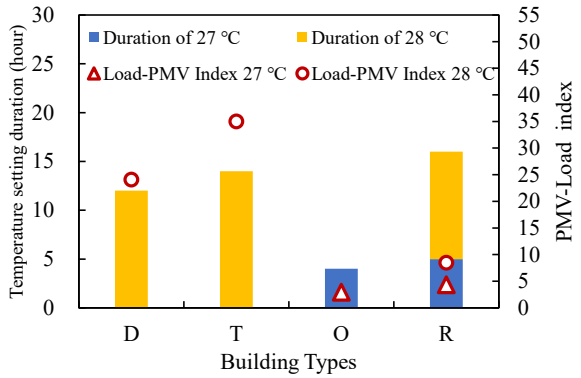

599
600 (a) PMV_10% scenario

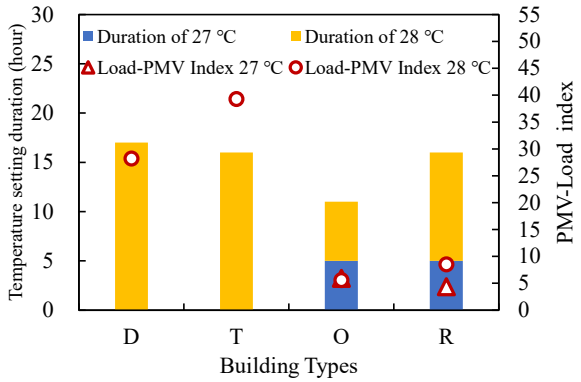

601
602 (b) PMV_20% scenario

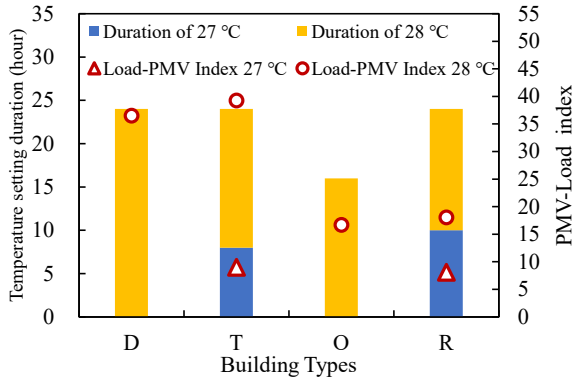

(c) PMV_30% scenario

Fig. 13 Load_PMV indexes under different scenarios

4.3 Optimal guidance considering the capita thermal comfort level

From the above analyses, the buildings and periods with higher cooling load reduction under the same PMV increase are adjusted preferential, which is quantified by the Load_PMV index. However, it was observed that these periods often had high occupancy, meaning that the indoor thermal environment was poor when most residents were present in the building. Therefore, the Load_Occ_PMV index is introduced to reflect the thermal comfort level per capita and is used as the optimization objective. More attention is paid when the occupancy is higher, which may result in a higher indoor thermal environment at occupant time. The Load_Occ_PMV index in different buildings is shown in Fig. 14. Compared with the Load_PMV index, the Load_Occ_PMV index is smaller when the occupancy is higher. The Load_Occ_PMV index for dormitory buildings and residential is lower at night. For office buildings, the index is lower in the daytime. For the teaching building, except during the load increase period, the index is higher during the daytime because there is no occupant at night. In summary, the Load_Occ_PMV index helps in prioritizing the adjustment of indoor temperature based on occupancy levels. It ensures that more emphasis is given to periods when more people are present, thereby improving the overall thermal comfort experience of occupants.

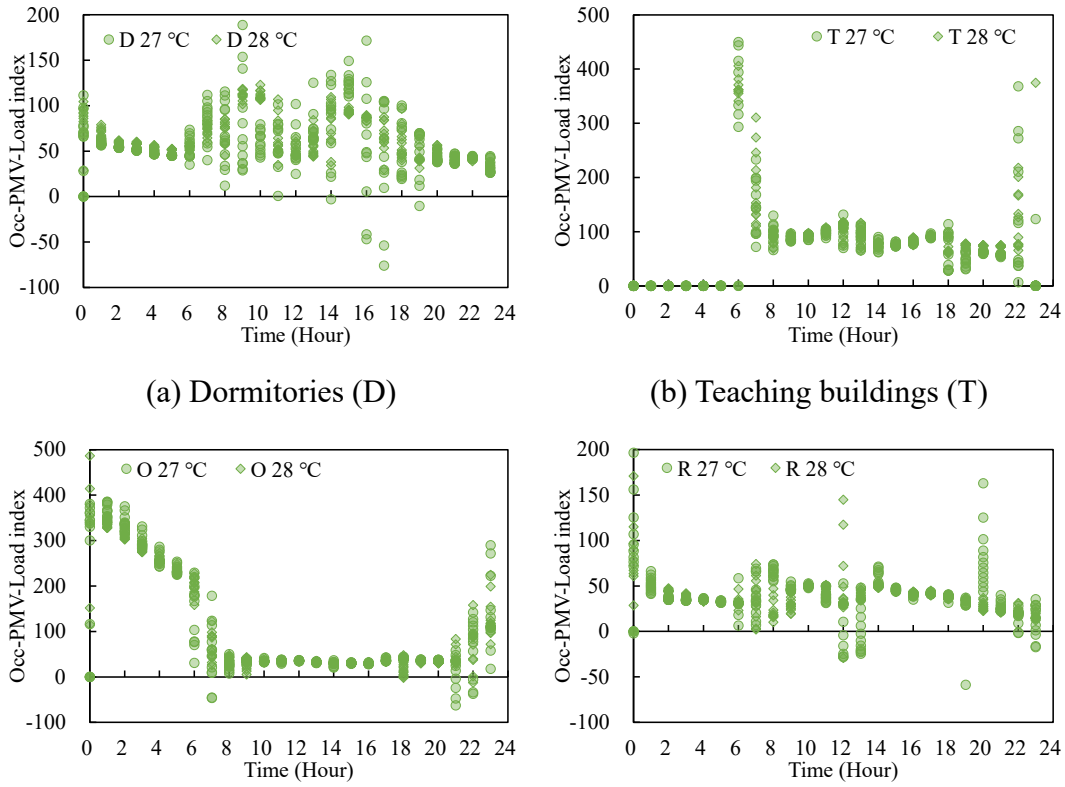

(a) Dormitories (D) (b) Teaching buildings (T)

(c) Office buildings (O) (d) Residential (R)

Fig. 14 Load_Occ_PMV index of four types of buildings under different indoor temperatures

The optimal temperature setting guidance using the Occ_PMV index is shown in Fig. 15, the trend is different from the results under the Load_PMV index. From the optimized indoor air temperature setpoints in Occ_PMV_10% scenario, the indoor air temperature in dormitories is increased to 28 ℃ during daytime and is reduced to 25 ℃ at night. In office buildings, the temperature is increased to 27 ℃ and 28 ℃ at night. The indoor thermal environment of these two types of buildings is guaranteed. However, to achieve the total carbon emission quota, the temperature is higher in the other two types of buildings. In teaching buildings, the temperature is increased to 28 ℃ in the daytime, despite the relatively high occupancy rate. The temperature of the residential buildings is increased to 27 ℃ at 8:00 and further increased to 28 ℃ at 14:00. With the increase of the carbon reduction target, the indoor temperature of all types of buildings is increased accordingly. In the Occ_PMV_20% and Occ_PMV_30% scenarios, the dormitory building experiences almost all-day temperatures of 28°C. As for teaching

buildings, due to the low Load_Occ_PMV index at night, the temperatures did not rise above 26 ℃ at night. In office buildings, the index is lower in the daytime, so the indoor temperature stays at 25 ℃. However, with the carbon limitation further increasing to 30%, the indoor temperature should be increased to 28 ℃ at most times of the day to ensure the carbon emission is within the quota. As for residential buildings, under the constraints of different levels of carbon quotas, the temperature setting of the day does not change much, and the indoor thermal environment at night can be ensured. This can be attributed to the fact that residential buildings have a lower Load_Occ_PMV index compared to the other building types, making temperature regulation for load reduction less critical.

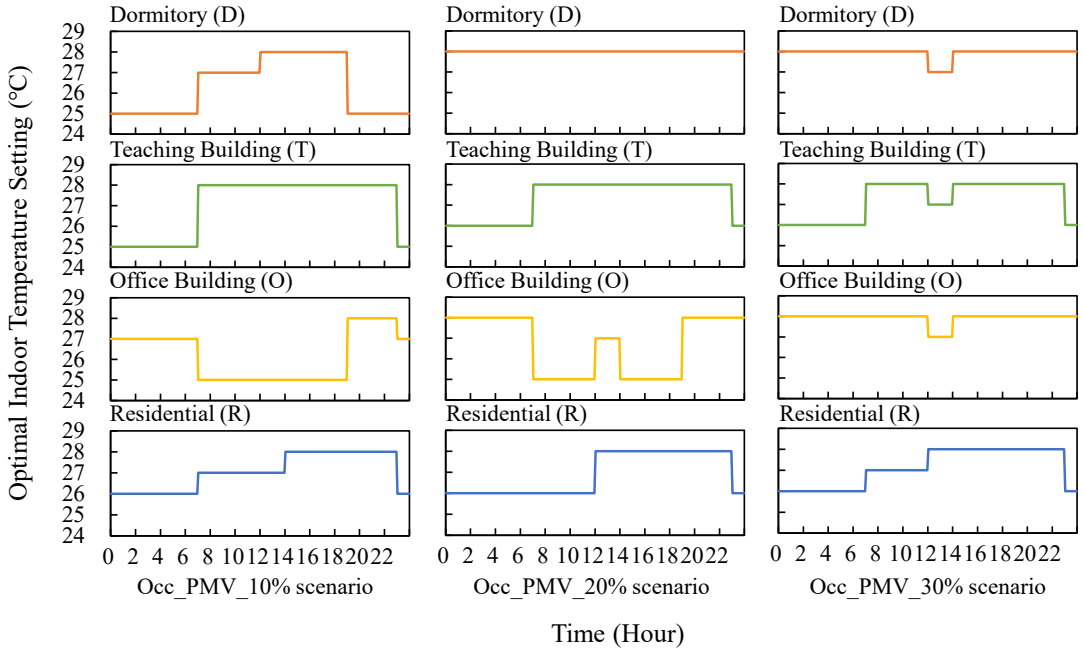

Fig. 15 Indoor temperature optimization results under Load_Occ_PMV index

The indoor thermal environment and system performance under the optimal temperature setting under the Load_PMV index and Load_Occ_PMV index are compared with the unified temperature settings. As shown in Fig. 16, comparing the indoor thermal environment under the Load_PMV index and the Load_Occ_PMV index, there is little difference in indoor thermal comfort under the same carbon emission quota. Using the Load_PMV index results in a lower average PMV value, but

the occupancy-weighted PMV (Occ_PMV) is higher. For instance, under the 20% cooling carbon reduction target, the average PMV by using the Load_PMV index is 0.46, which is lower than the PMV by using the Load_Occ_PMV index (0.52). However, the Occ_PMV is higher in the Occ PMV 20% scenario, indicating a higher average thermal environment during the occupants' time. From the perspective of system carbon emission, choosing different evaluation indexes as optimization goals has limited influence on the carbon emission of cooling systems. Under the 20% cooling carbon reduction target, the carbon emissions of cooling systems are nearly the same, and both are lower than the emission in scenario of 27 ℃. This result means under the optimal temperature settings, the occupant can get a higher indoor thermal environment under less system carbon emissions compared with the unified temperature setting.

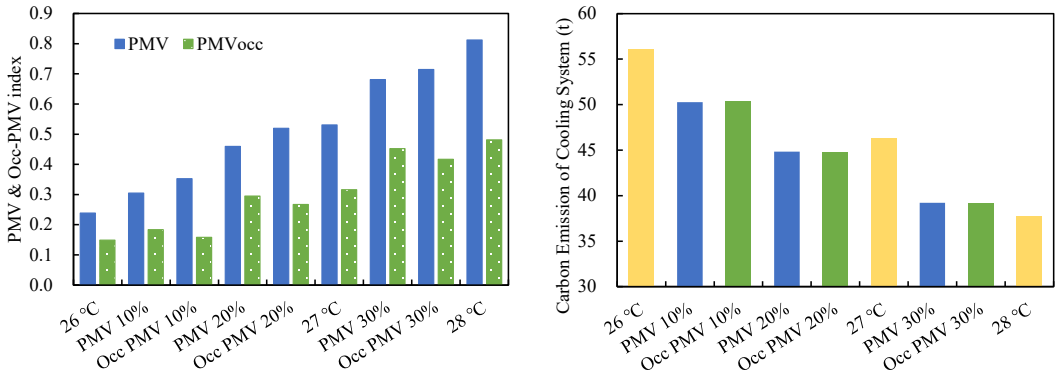

(a) Indoor thermal environment (b) Carbon emission

Fig. 16 Indoor thermal environment and carbon emission under two indexes

5 Discussion

This study focuses on demand response for distributed energy systems with multi-users for carbon reduction, efficiency improvement, and less impact on users. Although carbon emission reduction has been proposed for a long time, it seems that it is only related to the energy production side, and the direct relationship with consumers is not clear. Therefore, it is necessary to involve users in carbon reduction through demand response strategies to enhance their understanding of the effects of their behaviors. Therefore, it is necessary to provide simple, feasible, easy-to-operate, and low-impact

ways to promote user participation. Users can adjust the air conditioner themselves following the guidance provided by the aggregator, or authorize the aggregator to adjust it automatically. However, the study has limitations as it only considers the case of system carbon emission within the carbon quota, disregarding the economy of carbon trading, and building income. Particularly, when the system design changes (e.g., higher renewable energy capacity, smaller internal combustion engine capacity), the system becomes more integrated with the grid. The aim of the demand response may have to focus more on increasing the utilization ratio of renewable energy, reducing the peak demand from the grid or enhancing the economic performance of the participants and the DESs. Including these elements can broaden the application scope and yield more insightful results. In addition, the optimization process is hindered by the complexity of the system and building models, necessitating a balanced approach to address the trade-off between model complexity and optimization time. Future work will focus on exploring the economy aspects, simplifying models, and incorporating greater user diversity.

6 Conclusions

In this paper, a two-level collaborative demand-side management framework for distributed energy systems is proposed. The objective is to ensure that the system's carbon emissions are within the allocated quota while minimizing the thermal impact on occupants by providing optimal indoor temperature guidance. The optimal temperature settings are determined by taking into account the collaboration between the energy supply side and the demand side, as well as the collaboration between different users. Three levels of carbon quotas and two indoor thermal environment evaluation indexes are used in the case study. The following conclusions can be summarized:

- In the proposed two-level demand-side management framework, the optimal indoor temperature settings for various types of buildings are obtained under different levels of carbon quotas. Through the collaboration between the energy

supply side and the demand side, the system efficiency can be increased by up to 1.9%.

- Through collaboration between different users on the demand side, users can adjust the indoor temperature based on their load characteristics in the demand response with minimum overall thermal comfort impact. In PMV _20% scenario, compared with the 27 ℃ scenario, the optimal scenario can reduce carbon emissions by 1.66 t with 0.07 lower PMV.
- When using different indoor thermal environment evaluation indexes, the optimized temperature settings are both superior to uniform adjustment. Using the PMV index can achieve a lower average PMV for all types of buildings. The Occ-PMV index can achieve a higher indoor thermal environment during high occupant hours.
- The temperature settings of various types of builds at different times are related to the Load_PMV index and Load_Occ_PMV index. A higher index value refers to greater cooling reduction with less impact on the thermal environment and should be given priority in the demand response.

The proposed collaborative demand-side management framework can provide clear temperature-setting guidance for different types of buildings in distributed energy systems to meet specific carbon quotas. This study has positive significance for encouraging user participation in distributed energy systems and achieving energy saving and carbon reduction objectives.

Acknowledgement

The research presented in this paper is supported by the National Key Research and Development Program of China (2021YFE0107400).

Appendix A.

Table A1 Value of coefficients in the internal combustion engine model

plr	η_{ele}	η_{mec}	f_{jw}	f_{exh}	Fac_{exh}
0.40	0.425	0.989	0.155	0.559	0.398
0.50	0.438	0.996	0.179	0.539	0.474
0.60	0.448	0.997	0.200	0.522	0.559
0.70	0.453	0.996	0.222	0.505	0.653
0.75	0.454	0.992	0.243	0.490	0.716
0.80	0.453	0.988	0.264	0.476	0.782
0.90	0.452	0.984	0.283	0.462	0.887
1.00	0.445	0.980	0.302	0.451	1.000

738 Table A2 Value of coefficients in the absorption chiller model

Coefficients	Value	Coefficients	Value	Coefficients	Value
a_1	1.4196	b_1	-0.01069	c_1	-0.0021
a_2	-3.6846	b_2	0.24992	c_2	0.0911
a_3	3.8314	b_3	-0.22439	c_3	0.2350
a_4	-0.5630				

739 Table A3 Value of coefficients in the heat pump model

Coefficients	Value	Coefficients	Value	Coefficients	Value
e_1	1.0340	f_2	0.01914	g_1	0.8382
e_2	0.2508	f_3	0.00659	g_2	-0.0604
e_3	-0.2848	f_4	-0.09575	g_3	0.2203
f_1	0.58170	f_5	0.49110		

740

741 ## Reference

742 Afzalan, M., & Jazizadeh, F. 2019. Residential loads flexibility potential for demand
743 response using energy consumption patterns and user segments. Appl. Energy.
744 254, 113693.https://doi.org/10.1016/j.apenergy.2019.113693.
745 Aghniaey, S., & Lawrence, T. M. 2018. The impact of increased cooling setpoint
746 temperature during demand response events on occupant thermal comfort in
747 commercial buildings: A review. Energy Build. 173, 19-
748 27.https://doi.org/10.1016/j.enbuild.2018.04.068.
749 Alzahrani, A., Sajjad, K., Hafeez, G., Murawwat, S., Khan, S., & Khan, F. A. 2023.
750 Real-time energy optimization and scheduling of buildings integrated with
751 renewable microgrid. Appl. Energy. 335,
752 120640.https://doi.org/10.1016/j.apenergy.2023.120640.
753 Amin, U., Hossain, M. J., & Fernandez, E. 2020. Optimal price based control of HVAC
754 systems in multizone office buildings for demand response. J. Clean Prod. 270,
755 122059.https://doi.org/10.1016/j.jclepro.2020.122059.
756 Arteconi, A., Patteeuw, D., Bruninx, K., Delarue, E., D'haeseleer, W., & Helsen, L.

2016. Active demand response with electric heating systems: Impact of market penetration. Appl. Energy. 177, 636-648.https://doi.org/10.1016/j.apenergy.2016.05.146.

Azuatalam, D., Lee, W.-L., de Nijs, F., & Liebman, A. 2020. Reinforcement learning for whole-building HVAC control and demand response. Energy and AI. 2, 100020.https://doi.org/10.1016/j.egyai.2020.100020.

China, M. o. E. a. W. o. t. P. s. R. o. 2022. Notice on key work related to the reporting and management of enterprise greenhouse gas emissions in 2022. https://www.mee.gov.cn/xxgk2018/xxgk/xxgk06/202203/t20220315_971468.html.

Christantoni, D., Oxizidis, S., Flynn, D., & Finn, D. P. 2016. Implementation of demand response strategies in a multi-purpose commercial building using a whole-building simulation model approach. Energy Build. 131, 76-86.https://doi.org/10.1016/j.enbuild.2016.09.017.

Energy, U. S. D. o. 2006. Benefits of Demand Response in Electricity Markets and Recommendations for Achieving Them

Erdinç, O., Taşcıkaraoğlu, A., Paterakis, N. G., Eren, Y., & Catalão, J. P. S. 2017. End-User Comfort Oriented Day-Ahead Planning for Responsive Residential HVAC Demand Aggregation Considering Weather Forecasts. IEEE Trans. Smart Grid. 8, 362-372.https://doi.org/10.1109/TSG.2016.2556619.

Gao, Y., Li, S., Fu, X., Dong, W., Lu, B., & Li, Z. 2020. Energy management and demand response with intelligent learning for multi-thermal-zone buildings. Energy. 210, 118411.https://doi.org/10.1016/j.energy.2020.118411.

Guo, W., Wang, Q., Liu, H., & Desire, W. A. 2023. Multi-energy collaborative optimization of park integrated energy system considering carbon emission and demand response. Energy Rep. 9, 3683-3694.https://doi.org/10.1016/j.egyr.2023.02.051.

Hafeez, G., Alimgeer, K. S., Wadud, Z., Khan, I., Usman, M., Qazi, A. B., & Khan, F. A. 2020. An Innovative Optimization Strategy for Efficient Energy Management With Day-Ahead Demand Response Signal and Energy Consumption Forecasting in Smart Grid Using Artificial Neural Network. IEEE Access. 8, 84415-84433.https://doi.org/10.1109/ACCESS.2020.2989316.

Hoyt, T., Lee, K. H., Zhang, H., Arens, E., & Webster, T. 2005. Energy savings from extended air temperature setpoints and reductions in room air mixing

Huang, W., Zhang, N., Kang, C., Li, M., & Huo, M. 2019. From demand response to integrated demand response: review and prospect of research and application. Prot. Control Mod. Power Syst. 4, 12.https://doi.org/10.1186/s41601-019-0126-4.

ISO7730. 2005. "ISO 7730:2005 Ergonomics of the thermal environment — Analytical determination and interpretation of thermal comfort using calculation of the PMV and PPD indices and local thermal comfort criteria." In.

Jazzbin, e. a. 2020. geatpy: The genetic and evolutionary algorithm toolbox with high

performance in python. http://www.geatpy.com/.
Jin, X., Xiao, F., Zhang, C., & Chen, Z. 2022. Semi-supervised learning based framework for urban level building electricity consumption prediction. Appl. Energy. 328, 120210.https://doi.org/10.1016/j.apenergy.2022.120210.
Kirkerud, J. G., Nagel, N. O., & Bolkesjø, T. F. 2021. The role of demand response in the future renewable northern European energy system. Energy. 235, 121336.https://doi.org/10.1016/j.energy.2021.121336.
Li, A., Xiao, F., Zhang, C., & Fan, C. 2021. Attention-based interpretable neural network for building cooling load prediction. Appl. Energy. 299, 117238.https://doi.org/10.1016/j.apenergy.2021.117238.
Li, L., & Yu, S. 2020. Optimal management of multi-stakeholder distributed energy systems in low-carbon communities considering demand response resources and carbon tax. Sustain. Cities Soc. 61, 102230.https://doi.org/10.1016/j.scs.2020.102230.
Li, Y., Bu, F., Gao, J., & Li, G. 2022. Optimal dispatch of low-carbon integrated energy system considering nuclear heating and carbon trading. J. Clean Prod. 378, 134540.https://doi.org/10.1016/j.jclepro.2022.134540.
Mancarella, P., & Chicco, G. 2013. Real-Time Demand Response From Energy Shifting in Distributed Multi-Generation. IEEE Trans. Smart Grid. 4, 1928-1938.https://doi.org/10.1109/TSG.2013.2258413.
outlook, b. e. 2020. Statistical Review of World Energy. https://www.bp.com/en/global/corporate/energy-economics/statistical-review-of-world-energy.html.
Ran, F., Gao, D.-c., Zhang, X., & Chen, S. 2020. A virtual sensor based self-adjusting control for HVAC fast demand response in commercial buildings towards smart grid applications. Appl. Energy. 269, 115103.https://doi.org/10.1016/j.apenergy.2020.115103.
Romero Rodríguez, L., Sánchez Ramos, J., Álvarez Domínguez, S., & Eicker, U. 2018. Contributions of heat pumps to demand response: A case study of a plus-energy dwelling. Appl. Energy. 214, 191-204.https://doi.org/10.1016/j.apenergy.2018.01.086.
Sheikhi, A., Bahrami, S., & Ranjbar, A. M. 2015. An autonomous demand response program for electricity and natural gas networks in smart energy hubs. Energy. 89, 490-499.https://doi.org/10.1016/j.energy.2015.05.109.
Shi, B., Li, N., Gao, Q., & Li, G. 2022. Market incentives, carbon quota allocation and carbon emission reduction: Evidence from China's carbon trading pilot policy. J. Environ. Manage. 319, 115650.https://doi.org/10.1016/j.jenvman.2022.115650.
Smith, A. M., & Brown, M. A. 2015. Demand response: A carbon-neutral resource? Energy. 85, 10-22.https://doi.org/10.1016/j.energy.2015.02.067.
Su, Y., Zhou, Y., & Tan, M. 2020. An interval optimization strategy of household multi-energy system considering tolerance degree and integrated demand response.

Appl. Energy. 260, 114144.https://doi.org/10.1016/j.apenergy.2019.114144.
Tang, R., Wang, S., & Shan, K. 2018. Optimal and near-optimal indoor temperature and humidity controls for direct load control and proactive building demand response towards smart grids. Autom. Constr. 96, 250-261.https://doi.org/10.1016/j.autcon.2018.09.020.
the Solar Energy Laboratory, U. o. W.-M. a. T. E. S. S., LLC. 2017. "TRNSYS 18 Documentation Volume 4 Mathematical Reference." In.
Tian, Z., Fu, F., Niu, J., Sun, R., & Huang, J. 2019. Optimization and extraction of an operation strategy for the distributed energy system of a research station in Antarctica. J. Clean Prod., 119073.https://doi.org/10.1016/j.jclepro.2019.119073.
Wang, H., Wang, S., & Tang, R. 2019. Development of grid-responsive buildings: Opportunities, challenges, capabilities and applications of HVAC systems in non-residential buildings in providing ancillary services by fast demand responses to smart grids. Appl. Energy. 250, 697-712.https://doi.org/10.1016/j.apenergy.2019.04.159.
Wang, J., Zhong, H., Ma, Z., Xia, Q., & Kang, C. 2017. Review and prospect of integrated demand response in the multi-energy system. Appl. Energy. 202, 772-782.https://doi.org/10.1016/j.apenergy.2017.05.150.
Wang, J., Zhu, J., Ding, Z., Zou, P. X. W., & Li, J. 2019. Typical energy-related behaviors and gender difference for cooling energy consumption. J. Clean Prod. 238, 117846.10.1016/j.jclepro.2019.117846.
Weng, Z., Liu, T., Wu, Y., & Cheng, C. 2022. Air quality improvement effect and future contributions of carbon trading pilot programs in China. Energy Policy. 170, 113264.https://doi.org/10.1016/j.enpol.2022.113264.
Winstead, C., Bhandari, M., Nutaro, J., & Kuruganti, T. 2020. Peak load reduction and load shaping in HVAC and refrigeration systems in commercial buildings by using a novel lightweight dynamic priority-based control strategy. Appl. Energy. 277, 115543.https://doi.org/10.1016/j.apenergy.2020.115543.
Xiao, Z., Gang, W., Yuan, J., Chen, Z., Li, J., Wang, X., & Feng, X. 2022. Impacts of data preprocessing and selection on energy consumption prediction model of HVAC systems based on deep learning. Energy Build. 258, 111832.https://doi.org/10.1016/j.enbuild.2022.111832.
Yan, Q., Lin, H., Zhang, M., Ai, X., Gejirifu, D., & Li, J. 2022. Two-stage flexible power sales optimization for electricity retailers considering demand response strategies of multi-type users. Int. J. Electr. Power Energy Syst. 137, 107031.https://doi.org/10.1016/j.ijepes.2021.107031.
Yan, X., Ozturk, Y., Hu, Z., & Song, Y. 2018. A review on price-driven residential demand response. Renew. Sust. Energ. Rev. 96, 411-419.https://doi.org/10.1016/j.rser.2018.08.003.
Yang, P., Jiang, H., Liu, C., Kang, L., & Wang, C. 2023. Coordinated optimization scheduling operation of integrated energy system considering demand response

and carbon trading mechanism. Int. J. Electr. Power Energy Syst. 147, 108902.https://doi.org/10.1016/j.ijepes.2022.108902.

Yuan, J., Xiao, F., Gang, W., Zhang, Y., Shi, J., Zhang, Z., & Hao, X. 2023. Load allocation methods for the thermal and electrical chillers in distributed energy systems for system efficiency improvement. Energy Conv. Manag. 292, 117334.https://doi.org/10.1016/j.enconman.2023.117334.

Yuan, J., Xiao, Z., Chen, X., Lu, Z., Li, J., & Gang, W. 2021. A Temperature & Humidity Setback Demand Response Strategy for HVAC Systems. Sustain. Cities Soc., 103393.https://doi.org/10.1016/j.scs.2021.103393.

Zhang, S., Hu, W., Du, J., Bai, C., Liu, W., & Chen, Z. 2023. Low-carbon optimal operation of distributed energy systems in the context of electricity supply restriction and carbon tax policy: A fully decentralized energy dispatch strategy. J. Clean Prod. 396, 136511.https://doi.org/10.1016/j.jclepro.2023.136511.

Zhang, Y., Akkurt, N., Yuan, J., Xiao, Z., Wang, Q., & Gang, W. 2020. Study on model uncertainty of water source heat pump and impact on decision making. Energy Build. 216, 109950.https://doi.org/doi.org/10.1016/j.enbuild.2020.109950.

Zhou, X., Niu, A., & Lin, C. 2023. Optimizing carbon emission forecast for modelling China's 2030 provincial carbon emission quota allocation. J. Environ. Manage. 325, 116523.https://doi.org/10.1016/j.jenvman.2022.116523.

Zhu, G., & Gao, Y. 2023. Multi-objective optimal scheduling of an integrated energy system under the multi-time scale ladder-type carbon trading mechanism. J. Clean Prod. 417, 137922.https://doi.org/10.1016/j.jclepro.2023.137922.